Received: 21 October 2022 | Accepted: 8 March 2023

DOI: 10.1111/jfb.15374

REGULAR PAPER

JOURNAL OF FISH BIOLOGY fsbi

Age, growth and maturity of the yellow stingray (*Urobatis jamaicensis*), a biannually reproductive tropical batoid

Jessica J. Schieber[1] | Daniel P. Fahy[1] | John K. Carlson[2] | David W. Kerstetter[1]

[1]Halmos College of Arts and Sciences, Nova Southeastern University, 8000 North Ocean Drive, Dania Beach, Florida, 33004, USA

[2]National Oceanic and Atmospheric Association, National Marine Fisheries Service, 3500 Delwood Beach Road, Panama City, Florida, 32408, USA

Correspondence
David W. Kerstetter, Halmos College of Arts and Sciences, Nova Southeastern University, 8000 North Ocean Drive, Dania Beach, Florida, 33004, USA.
Email: kerstett@nova.edu

Present address
Jessica J. Schieber, Florida Fish and Wildlife Conservation Commission, Fish and Wildlife Research Institute, 1220 Prospect Avenue #285, Melbourne, Florida, 32901, USA.

Abstract

Urobatis jamaicensis is a coastal batoid species affected by habitat loss and small-scale exploitation from fisheries and the aquarium trade, yet the life-history information available is limited. This is the first study to assess the vertebral centra from 195 stingrays to estimate age and growth patterns, and compare them with the biannual reproductive pattern previously reported for this species. Age-at-size data were compared using five different growth models and found a two-parameter von Bertalanffy growth function (VBGF), the Gompertz model and a modified VBGF fit best for males, females and sexes combined, respectively. Maturity was achieved before 1 year. However, growth did not cease with the onset of maturity, but instead slowed down. Results from marginal increment analysis and edge analysis indicated a nonannual somatic growth pattern with influences from the biannual reproduction cycle where peaks in resource allocation may be focused on ovulation rather than growth during March when larger brood sizes are present, while resources may be allocated more towards growth during August and September when brood sizes are generally smaller. These results may be used as a proxy for species with similar reproductive patterns or for those that lack annual or seasonal growth patterns.

KEYWORDS
batoids, biannual reproduction, greater Caribbean, Urotrygonidae, von Bertalanffy

1 | INTRODUCTION

Age determination and validation studies have become increasingly important in fisheries management policies for the conservation of elasmobranch species. Most elasmobranchs are characterized as K-selected species due to their slow growth, prolonged maturation periods, lengthy lifespans, infrequent reproduction and low fecundity, making them vulnerable to overfishing and habitat degradation (Matta *et al*., 2017). Batoids are especially susceptible to fishing activities along the continental shelf (Oliver *et al*., 2015) and account for roughly 36% of catches within the western Atlantic Ocean, predominantly as bycatch in small-scale industrial and artisanal trawl and gillnet fisheries (Ferrette *et al*., 2019). Conservation efforts are often aimed at species with an immediate risk of extinction, but it is vital to obtain the life-history information for all species, especially those within nearshore, tropical or subtropical environments where habitat degradation is high and exploitation is more frequent (Dale & Holland, 2012; Dulvy *et al*., 2014). Understanding the population dynamics of nonexploited species not only contributes to the management of targeted species but can indicate how natural populations are influenced and provide valuable information for ecosystem-based management plans (Green *et al*., 2009).

Hard-part age-estimation techniques are widely used for studying life-history patterns in fishes and has become pertinent in determining population dynamics relative to fishing pressures worldwide (Cailliet, 2015). The vertebrae of elasmobranchs are calcified structures

that accumulate growth material typically identified as opaque and translucent bands along the vertebral centra. Seasonal band deposition is characterized by thick opaque bands typically associated with faster growth during the summer (or warmer) months and narrow translucent bands that represent slower growth during the winter (or cooler) months (Cailliet & Goldman, 2004; Christiansen *et al*., 2016). However, the interpretation of band pair deposition can be influenced by the presence of nonannual growth marks, such as double-banding patterns, or through factors such as somatic growth rather than seasonal growth, as seen in species like the Pacific angel shark (*Squatina californica*; Natanson & Cailliet, 1990), basking shark (*Cetorhinus maximum*; Natanson *et al*., 2008) and wobbegong sharks (*Orectolobus ornatus*, *O. maculatus* and *O. halei*; Huveneers *et al*., 2013). Age-estimation studies of fishes and elasmobranchs primarily rely on the verification of annual growth band formation with two of the more common and easily accessible methods: edge analysis and marginal increment analysis (Cailliet, 1990; Campana, 2014; Matta *et al*., 2017; Okamura *et al*., 2013; Okamura & Semba, 2009). Edge analysis involves the identification of the last growth band present, while marginal increment analysis incorporates measurements of the last two individual growth bands. Both methods are plotted individually against the month of capture to determine the timing of growth band formation. In addition to verification, growth models are used to determine the growth parameters necessary for management decisions. The use of multiple growth models provides a better approach for estimates of several different parameters that are typically unavailable [*e.g*., estimated size at birth (L_0), asymptotic size (L_∞) or the maximum attainable size for individuals] and lowers the risk of yielding biologically unrealistic growth estimates (Katsanevakis & Maravelias, 2008; Smart *et al*., 2016).

The yellow stingray, *Urobatis jamaicensis* (Cuvier, 1816), is a coastal species with limited life-history information, especially regarding its age and growth patterns (Spieler *et al*., 2013; Sulikowski, 1996; Yañez-Arancibia & Amezcua-Linares, 1979). The yellow stingray is a small-sized ray of the family Urotrygonidae. It is identified by rounded pectoral fins, a well-developed caudal fin and a distinctive green or brown colour with patterns of yellow, gold and white spots (Fahy, 2004). The species occurs within the central western Atlantic and is dispersed in tropical and subtropical waters throughout most of the Greater Caribbean basin, with populations distributed along the coast of south-east Florida, portions of the Gulf of Mexico, northern South America and other Caribbean regions surrounding Cuba (Fahy *et al*., 2007; Spieler *et al*., 2013; Ward-Paige *et al*., 2011). In south-east Florida, *U. jamaicensis* exhibits a biannual reproductive cycle with ovulation coinciding with parturition and occurring between January and April and again from July to October. Gestation is *ca*. 5 months long based on patterns of embryonic development and the range in ovulation and parturition during consecutive, overlapping reproductive cycles (Fahy, 2017; Fahy *et al*., 2007).

American round stingrays (Urotrygonidae) are small to moderate-sized rays that are generally abundant and distributed nearshore in coastal waters, where they are often exposed to habitat degradation and fisheries activities (Dulvy *et al*., 2014; Kyne *et al*., 2012). Urotrygonids are not harvested commercially for food but are exploited through the aquarium trade and are highly vulnerable to artisanal fisheries, where they are frequently discarded as bycatch and susceptible to population decline (Dulvy *et al*., 2014; Mejía-Falla *et al*., 2014; Ward-Paige *et al*., 2011). Obtaining life-history information from *U. jamaicensis* is necessary for regions where it may already be impacted, and such methods can prove useful for similar species that are data deficient. The objective of this study was to increase the life-history information for the subtropical batoid species *U. jamaicensis* using the combination of age, growth and maturity estimates obtained from the south-east Florida population. Age estimates were determined from band pair counts along the radius of the vertebral centra, which were subsequently compared and verified with the biannual reproductive cycle.

2 | MATERIALS AND METHODS

A total of 195 specimens was collected from hard-bottom reef habitats throughout south-east Florida (Supporting Information Figure S1). Stingrays were collected *via* SCUBA using hand-nets and stored in mesh collection bags until euthanized by anaesthetic overdose *via* submersion in 500 mg $^{-1}$ MS-222 solution. Between 2003 and 2009, 165 individual yellow stingrays were collected (archived samples) with an additional 30 specimens collected during 2019 from the same area. For all specimens, morphometric measurements were recorded to the nearest millimetre with disc width (DW) measured at the widest point of the pectoral fins and total length (TL) measured from the tip of snout to the posterior edge of caudal fin (Ainsley, 2009; Başusta & Aslan, 2018). Total mass (TM) was recorded to the nearest gram (g) and compared with DW using a nonparametric regression due to the relatively small sample size. DW was used in place of TL for all analyses as stingray tails may appear truncated or damaged on capture.

For male specimens, the clasper length (CL) from the inferior margin of the cloacal slit to the tip of both claspers was measured to the nearest tenth of a millimetre. The average length between the left and right clasper was used for all analyses. To determine the best model fit, a nonlinear regression model for the combined means of the right and left clasper length versus DW was run to visualize the relationship. Male maturity was estimated following Fahy (2017) along with inspection of clasper calcification level (*i.e*., flexible or rigid). Maturity stages for females were recorded following Fahy (2017), while maternity status for females was noted when embryos were present or when recent parturition was evident. Maturity ogives, or the median DW at first maturity (DW_{50}), for both males and females and median DW at first maternity (DW_{50M}) for females were calculated using R software (v. 1.1.463; TeamRStudio R, 2018) following a binomial logistic regression. Ogives were fit using maximum likelihood with the following equation (Coelho & Erzini, 2005; Cotton *et al*., 2011; Mejía-Falla *et al*., 2014):

$$PA_i = \frac{1}{1 + e^{-b(A_i - A_{50})}}$$

where PA_i is the proportion of mature individuals at the *i*th size class, *b* is a model parameter, A_i is the size class and A_{50} is the median size

at which 50% of individuals are mature. Age-at-first maturity (A_{50}) and age-at-first maternity (A_{50M}) were determined following the same binomial regression, replacing size with age for A_{50}.

Vertebral columns extending from the occiput to the pelvic girdle were excised and soft tissues were removed and stored frozen prior to further cleaning and processing using the methods of Parsons *et al.* (2018). Subsequent to the cleaning process, three centra were selected and individually separated from the thoracic region of the vertebral column, where centra are largest along the vertebral column to maintain homogeneity between samples (Natanson *et al.*, 2008; Natanson, Andrews, *et al.*, 2018; Torres-Palacios *et al.*, 2019). Centra samples were sectioned along the sagittal plane using an Isomet-type low-speed diamond wheel saw (model 650; South Bay Technology Inc., San Clemente, CA, USA) to a range of thickness between 0.3 and 0.5 mm (depending on the size of centra) and viewed with a stereomicroscope (Olympus SZX2-ILLT; Olympus Corporation, Tokyo, Japan). Digital images were captured with an AmScope MU100 10MP digital microscope camera and computer software (v.x64, 3.7.10246, 2003–2017; AmScope, Irvine, CA, USA) (Campana, 2014; Hayne *et al.*, 2018). All images were digitally enhanced with Adobe Photoshop (v.21 2 January 2004) to adjust the contrast, light and sharpness for superior visualization of growth bands (McAuley *et al.*, 2006; Natanson, Skomal, *et al.*, 2018).

Three individual readers performed blind counts of all centra images twice to obtain a total of six counts for each sample. Age estimates were only accepted if four of the six counts were in agreement; all remaining samples were rejected (McAuley *et al.*, 2006). Samples were also discarded if double banding patterns or damage within the intermedialia was noted (Figure 5b,c). The accuracy and precision of age estimates were determined using percentage agreement:

$$\mathrm{PA} = \left[\frac{\text{no. agreed}}{\text{no. read}}\right] \times 100$$

in conjunction with average percentage error (APE):

$$\mathrm{APE}_j = 100\% \times \frac{1}{R}\sum_{i=1}^{R}\frac{|x_{ij} - X_j}{X_j}$$

where X_{ij} is the ith age determination of the jth fish, X_j is the mean age estimate of the jth fish and R is the number of times each fish is aged. The average coefficient of variation (ACV) was calculated:

$$\mathrm{CV}_j = 100\% \times \frac{\sqrt{\sum_{i=1}^{R}\frac{(X_{ij}-X_j)^2}{R-1}}}{X_j}$$

where CV_j is the age precision estimate for the jth fish (Campana, 2001). This was done both between readers with incremental size classes of 45 mm DW and between readers for all age classes combined (Campana *et al.*, 1995; Davis *et al.*, 2007; Natanson, Skomal, *et al.*, 2018). Systematic reader biases and the symmetry of band pair counts (age-estimates) were assessed using the McNemar test, Evans-Hoenig test, Bowker test and an age bias plot (Bowker, 1948; Cailliet & Goldman, 2004; Evans & Hoenig, 1998; Hale *et al.*, 2006; McNemar, 1947; Natanson *et al.*, 2014). (For a detailed description of all three tests used to assess the symmetry of band pair counts, see Evans & Hoenig, 1998.) All statistical analyses were performed with R statistical software (v. 1.1.463; TeamRStudio R, 2018) using the FSA and FSAData packages. Sectioned and whole vertebrae from each specimen were deposited in the Nunnally Fish Collection at the Virginia Institute of Marine Science (VIMS; Gloucester Point, Virginia, USA) under catalogue numbers VIMS_45268 to VIMS_45462.

Growth bands were verified using marginal increment analysis (MIA) (Lessa *et al.*, 2006; Okamura & Semba, 2009). The distance between the central point of the centra to the outer edge was recorded as the vertebral radius (μm) (Figure 5a). For each vertebral centra processed, the vertebral radius (V_R), the radius of the ultimate band (R_n) deposited and the radius of the penultimate band (R_{n-1}) deposited were measured digitally using ImageJ software (v.1.53; Abràmoff *et al.*, 2004; Schneider *et al.*, 2012) and applied to the following equation (Cotton *et al.*, 2011; Fernandez-Carvalho *et al.*, 2011):

$$\mathrm{MIA} = \frac{V_R - R_n}{R_{n-R_{n-1}}}$$

The resulting values were then plotted against the month of capture to estimate the rate of band formation (Cailliet *et al.*, 2006; Lessa *et al.*, 2006). Young of the year (YOY) were excluded from MIA as only the birth band was present along the vertebral centra. An ANOVA was used to determine if there were statistical differences between months with use of a Tukey pairwise comparison when normality assumptions were met, while a nonparametric Kruskal–Wallis test was used when homogeneity assumptions were not met to establish if any significant differences between months were present. The relationship between the vertebral radius (V_R) and DW was tested using a nonparametric regression. During edge analysis, the ultimate band was identified (opaque or translucent) by two readers with no prior knowledge of sample size, sex or age and compared to month of capture to determine frequency of edge type.

Various growth models were fit to DW-at-age data following Cailliet *et al.* (2006), Cotton *et al.* (2011) and Dale and Holland (2012). The von Bertalanffy growth function (VBGF) generates a growth curve that represents the predicted pattern of growth based on the following equation (Von Bertalanffy, 1938):

$$\mathrm{DW}_t = \mathrm{DW}_\infty - (\mathrm{DW}_\infty - \mathrm{DW}_0)e^{-kt}$$

where DW_t is the predicted disc width at age t, DW_∞ is the theoretical maximum mean DW ($t = \infty$), DW_0 is the estimated width at birth ($t = 0$) and k (year^{-1}) is the growth coefficient or the average rate at which the organism in a population will achieve the maximum DW (Cailliet & Goldman, 2004; Sulikowski, 1996).

Two variations of the VBGF were also compared to determine which model best represents the size-at-age data. The first variation of the VBGF model is a 'modified' form ($\mathrm{VBGF}_{\mathrm{mod}}$):

$$DW_t = DW_\infty\left(1 - e^{-k(t-t0)}\right)$$

where t_0 is the theoretical age when the DW is to zero. The second variation of the VBGF model is a two-parameter form ($VBGF_{2par}$) with a fixed DW-at-birth (DW_e) using the mean DW of term embryos, allowing for more variance at age-0:

$$DW_t = DW_\infty - (DW_\infty - DW_e)e^{-kt}$$

DW-at-birth was set at 83.0 mm for the $VBGF_{2par}$ derived from the term embryos sized in Fahy (2017). Lastly, a form of the Gompertz model (Mollet *et al*., 2002) was used for comparisons:

$$DW_t = DW_0 e\left(G\left(1 - e^{-kt}\right)\right)$$

where $G = \ln(DW_\infty/DW_0)$ and a logistic function where a is the inflexion point of the curve:

$$DW_t = DW_\infty/\left(1 + e^{-k(t-a)}\right)$$

All growth models were fitt using nonlinear least-squares (LS) and maximum likelihood estimation (ML) with R statistical software using the lme4, car and vbmodel libraries in R (v. 1.1.463; TeamRStudio R, 2018; Cotton *et al*., 2011; O'Shea *et al*., 2013). Both methods of model fitting were used to determine best fit as one method may provide additional information over the other when size-at-age data is limited, such as with the lack of an asymptote (LS) or for nonlinear data and small sample sizes (ML) (Cotton *et al*., 2011). Akaike information criterion (AIC) analysis was used to determine which growth model would yield the best fit for the DW-at-age data for least-squares regressions, while ML estimation used a form of AIC (AICc) with adjustment for small-sample biases (Charvet *et al*., 2018; Cotton *et al*., 2011; Gianeti *et al*., 2019).

3 | RESULTS

Female sizes ranged from 87 to 241 mm DW (mean ±s.d., 191.53 ± 22.95 mm, $n = 121$), 153 to 448 mm TL (356.78 ± 48.97 mm, $n = 121$) and 37 to 800 g TM (472.94 ± 159.06 g, $n = 121$). Male sizes ranged from 85 to 216 mm DW (179.53 ± 46.26 mm, $n = 74$), 151 to 398 mm TL (335.55 ± 46.26 mm, $n = 74$) and 37 to 612 g TM (382.23 ± 105.03 g, $n = 74$) (Figure 1). Females occurred more frequently, with an overall sample size of $n = 121$ (62%), whereas males were less frequently observed, with a sample size of $n = 74$ (38%). Specimens captured between 2003 and 2009 ($n = 165$) were targeted towards

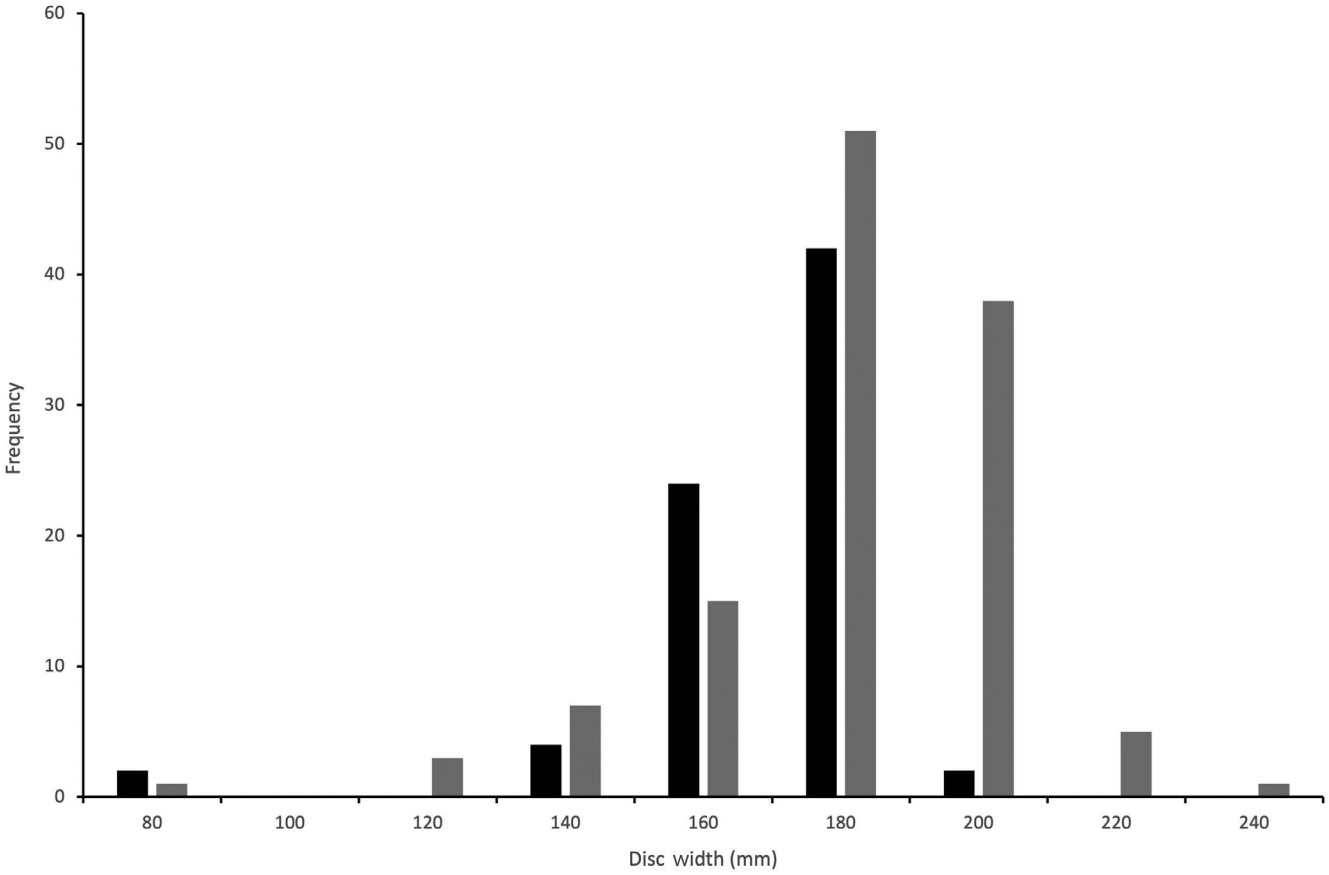

FIGURE 1 Disc width frequency distribution of male ($n = 74$) and female ($n = 121$) yellow stingray *Urobatis jamaicensis* caught between 2003 and 2019 in the western North Atlantic Ocean from sandy hard-bottom reefs in south-east Florida. ■, male; ■, female

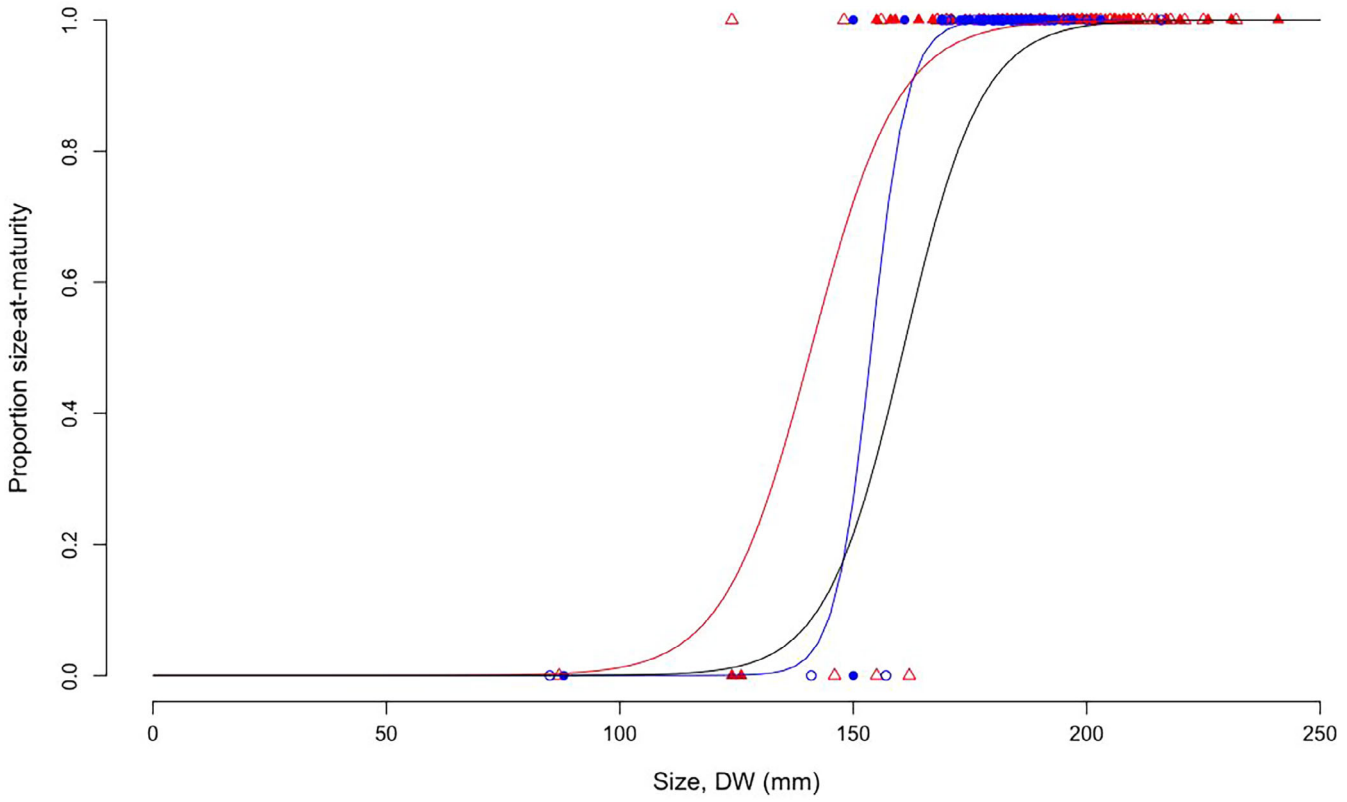

FIGURE 2 Size-at-maturity ogives for male ($n = 74$) and female ($n = 121$) yellow stingray *Urobatis jamaicensis* with female size-at-maternity ogives included. ○, immature males; ●, mature males; △, immature females; ▲, mature females; ——, female maternity

females, whereas specimens collected during 2019 ($n = 30$) were captured based on occurrence and did not statistically deviate from the 1:1 (male:female) ratio (chi-squared test, $\chi^2 = 0.133$, $P = 0.715$). During the 2019 collection, no term-stage embryos were present, although three neonates were caught in July (2019) and measured at 85 mm DW (151 mm TL), 87 mm DW (153 mm TL) and 88 mm DW (158 mm TL).

Nonparametric regressions indicated a statistically significant relationship between DW and TM for both sexes (males: TM $= -721.36 + 6.14 \times$ DW, P 0.01; females: TM $= -889.16 + 7.09 \times$ DW, $P < 0.01$) (Supporting Information Figure S2). The CL had a significant four-parameter logistic relationship to DW as indicated through a nonlinear regression where the inflexion point occurred at 155 mm DW (SE = 0.255, d.f. = 70, $P < 0.001$) (Supporting Information Figure S3).

Maturity ogives for size-at-first maturity (DW_{50}), age-at-first maturity (A_{50}) and size or age-at-first maternity (DW_{50M}, A_{50M}) were assessed using binomial regression. Males were sexually mature at 154 mm DW or 0.69 years [97.5% confidence interval (CI) = 0.107–0.684]. Females were sexually mature at 150 mm DW or 0.63 years (97.5% CI = 0.725–2.432). Female size at first maternity was 161 mm DW or 0.86 years (97.5 CI = 0.239–1.150) (Figures 2 and 3).

The relationship for DW and V_R was also found to be statistically significant through nonparametric regressions (males: $V_R = -4.36 + 0.17 \times$ DW, $P < 0.01$; females: $V_R = -2.88 + 0.11 \times$ DW, $P < 0.01$) (Figure 4). A total of 134 vertebral samples were processed for age determination analysis, with 61 (31.28%) of the original 195 discarded. Age estimates ranged from 0 to 5 years and 0 to 6 years for males and females, respectively. All three tests of symmetry (McNemar, Evans–Hoenig and Bowker) indicated there were no significant deviations from the final age for all three readers ($P > 0.01$) (Supporting Information Figure S4). Reader 2 showed slight overestimation for age 2 with underestimation at age 6, while reader 3 indicated slight underestimation for ages 4 and 4.

There was no statistical evidence of biases, with a strong relationship between the final age and initial age estimates assigned by the readers. All readers had an ACV value ≤6.4% and an APE ≤4.5%. When samples were separated into 45 mm DW classes (85–130 mm, 131–175 mm, 176–220 mm and 221–265 mm DW), all three tests of symmetry further indicated no systematic biases ($P > 0.01$) (Supporting Information Figure S5). The MIA measurements showed no distinct trends in growth over the course of the year (0.725 ± 0.353 mm, $n = 190$; Kruskal–Wallis, $P = 0.173$) (Supporting Information Figure S6). Mean MIAs were calculated from 190 *U. jamaicensis* samples collected between 2003 and 2019, with YOY ($n = 5$) excluded from analyses. Samples separated by age classes (1–2 bands, 3–4 bands and 5+ bands) for MIA yielded no statistically distinct trends in growth (ANOVA, $F_{10,23} = 0.62$, $P = 0.78$; ANOVA, $F_{11,66} = 1.20$, $P = 0.3$; ANOVA, $F_{8,7} = 1.01$, $P = 0.50$) (Supporting Information Figure S7). Samples separated by size classes (120–

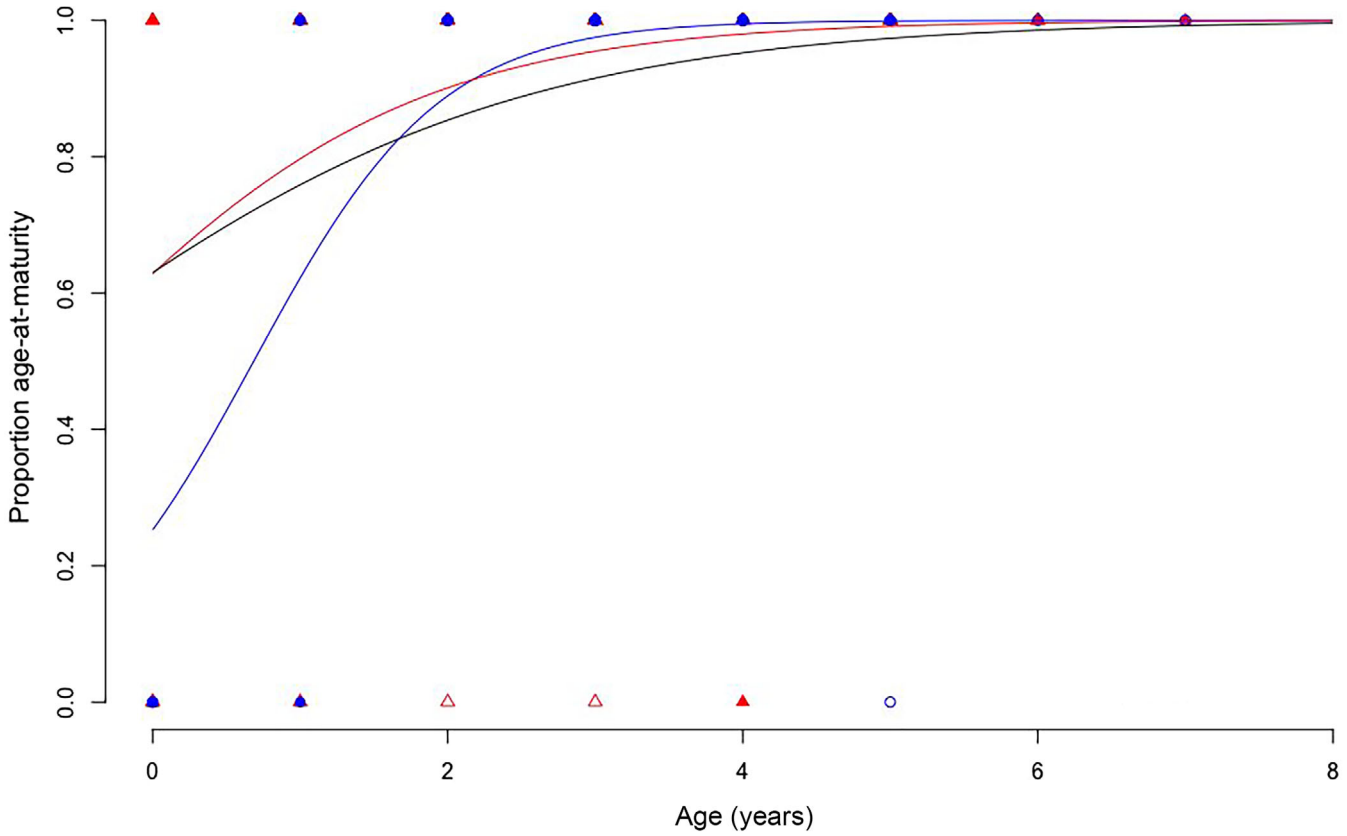

FIGURE 3 Age-at-maturity ogives for male ($n = 74$) and female ($n = 121$) yellow stingray *Urobatis jamaicensis* with age-at-maternity ogives included. ○, immature males; ●, mature males; △, immature females; ▲, mature females; ——, female maternity

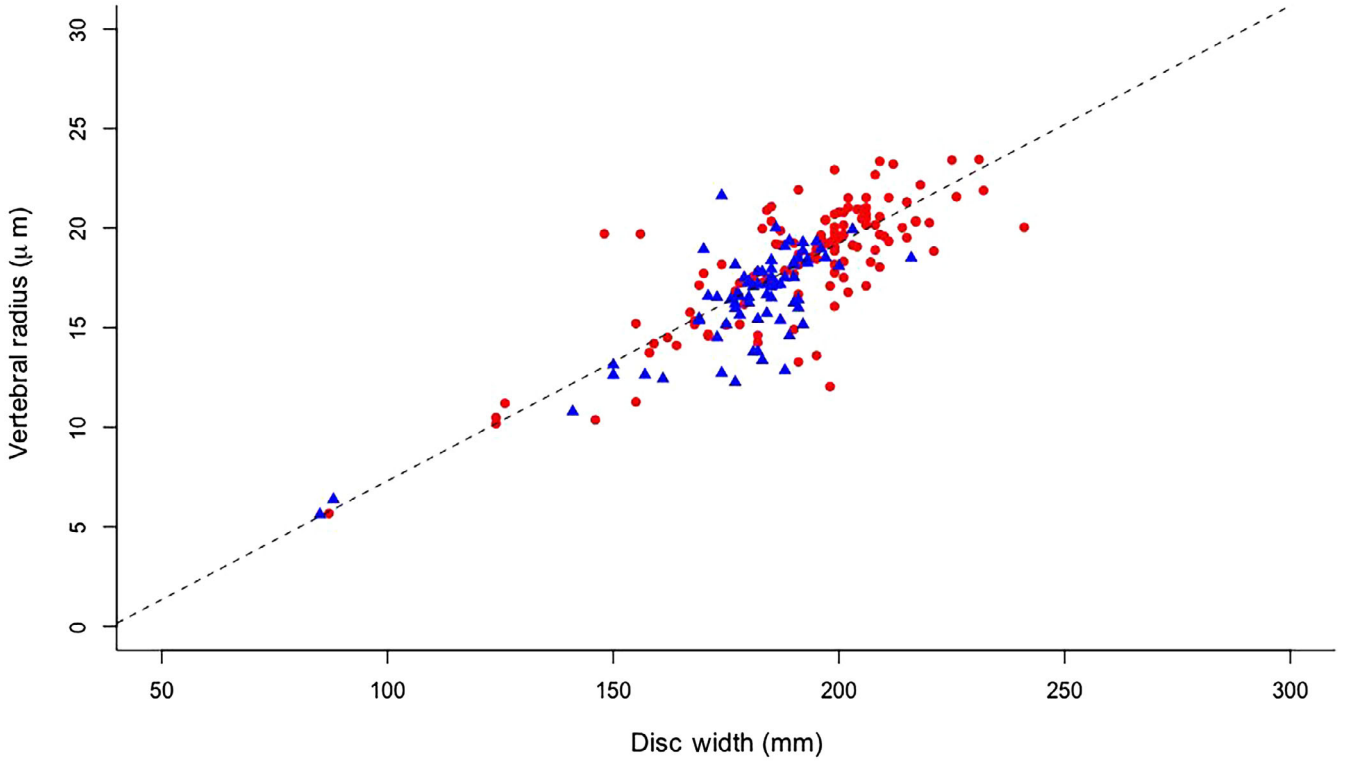

FIGURE 4 Nonparametric relationship between V_R (μm) and DW (mm) by sex for yellow stingray *Urobatis jamaicensis* ($n = 195$). ▲, female; ●, male

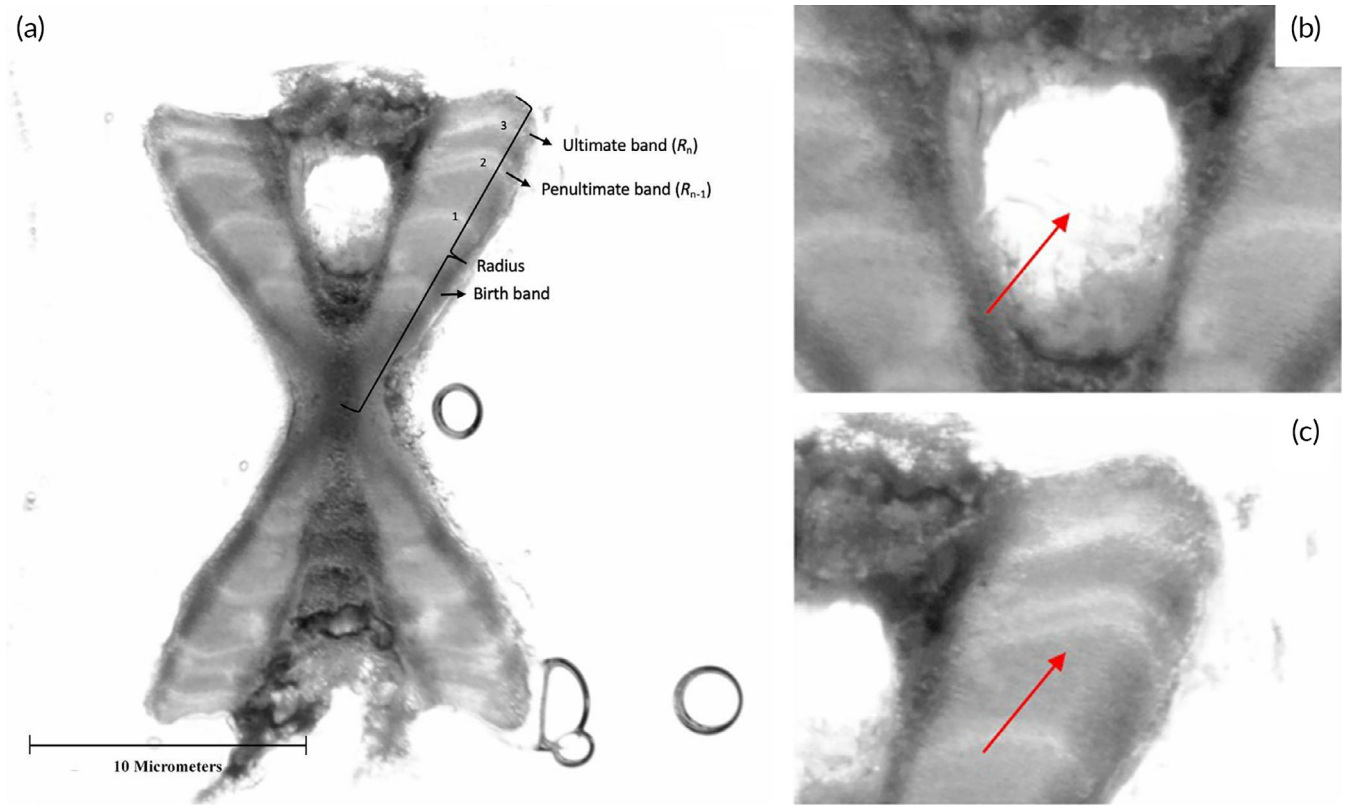

FIGURE 5 Image of vertebral centra (a) displaying readable bands on both sides of corpus calcareum that also displays (b) damage to the intermedialia and (c) double banding patterns

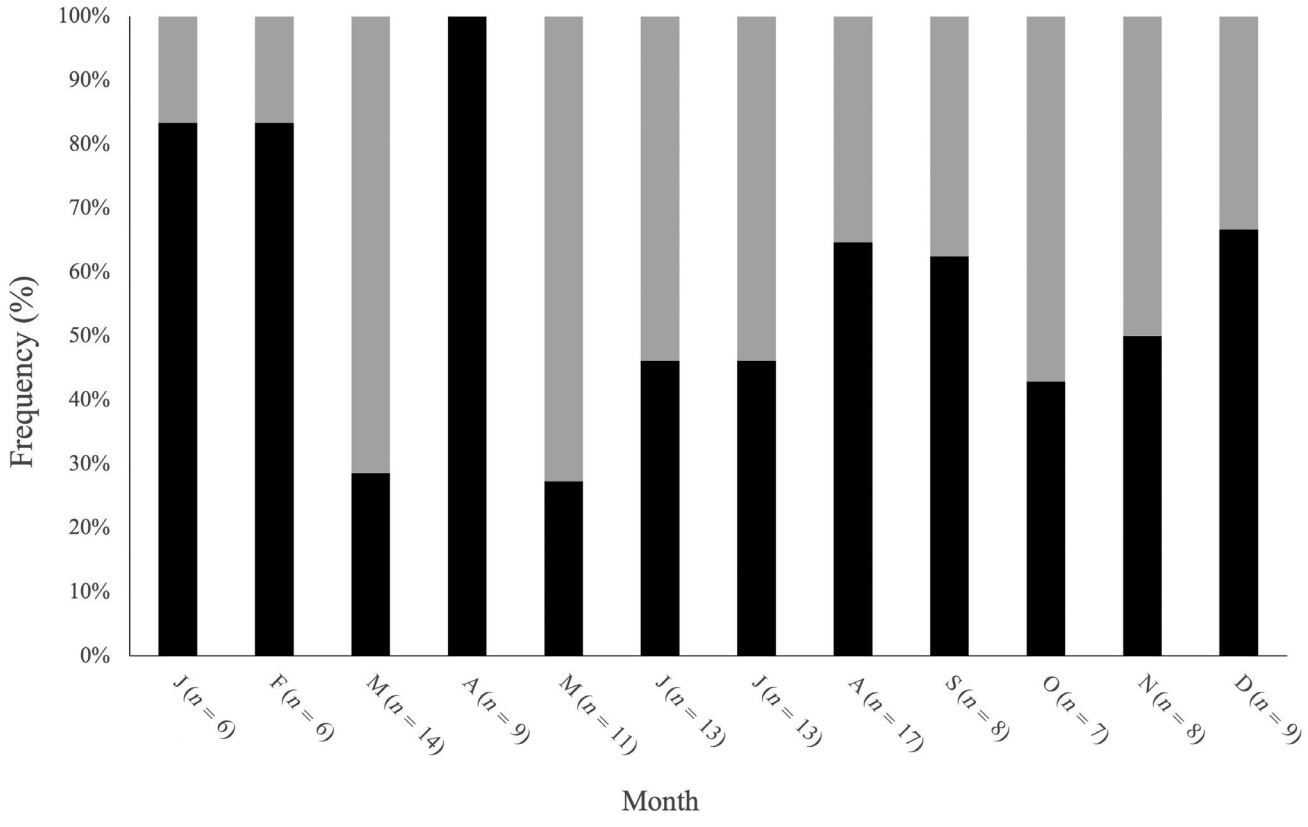

FIGURE 6 Monthly variation in formation of outer edge band type for yellow stingray *Urobatis jamaicensis* ($n = 121$). ■, opaque; ■, translucent

TABLE 1 Estimates of model parameters, standard deviation (σ, for ML-fitted models), residual sum of squares (RSS, for LS-fitted models) and model selection statistics (ΔAICc) for DW-at-age data for yellow stingray *Urobatis jamaicensis*

		Maximum likelihood						Least-squares regression					
Sex	**Model**	**DW_∞ (mm)**	**k (year^{-1})**	**DW_0 (mm)**	**t_0 (mm DW)**	**σ**	**ΔAICc**	**DW_∞ (mm)**	**k (year^{-1})**	**DW_0 (mm)**	**t_0 (mm DW)**	**RSS**	**ΔAICc**
SC	VBGF	194.44	77.84	120.99	–	18.5	14.489	194.44	1.15	121.72	–	41,192.61	0
	$VBGF_{mod}$	190.08	1.15	–	−0.85	17.53	0	194.44	1.15	–	−0.85	41,192.61	0
	Gompertz	132.13	1.32	121.84	–	17.55	0.268	193.95	1.32	121.82	–	41,274.99	0.2677
	$VBGF_{2par}$	190.08	25.33	–	–	20.18	35.535	193.2	1.62	–	–	50,089.35	25.084
	Logistic	193.55	1.51	–	−0.35	17.57	0.529	193.55	1.51	–	−0.35	41,355.53	0.529
Male	VBGF	184.05	2.16	86.57	–	9.26	2.0973	184.05	2.16	86.58	–	4028.863	2.0973
	$VBGF_{mod}$	184.05	2.16	–	−0.29	9.26	2.0973	184.05	2.16	–	−0.29	4028.863	2.0973
	Gompertz	176.29	2.55	86.58	–	9.27	2.1823	183.91	2.55	86.47	–	4036.155	2.1823
	$VBGF_{2par}$	184.03	2.21	–	–	9.29	0	184.03	2.21	–	–	4054.395	0
	Logistic	183.83	2.97	–	0.04	9.27	2.2443	183.83	2.97	–	0.04	4041.481	2.2443
Female	VBGF	201.64	0.83	138	–	18.25	0.0026	201.53	0.83	137.84	–	43,243.95	0.0031
	$VBGF_{mod}$	201.53	0.83	–	−1.38	18.25	0.0035	201.53	0.83	–	−1.38	43,243.95	0.0031
	Gompertz	201.24	0.95	137.77	–	18.24	0	200.93	0.94	137.96	–	43,256.13	0
	$VBGF_{2par}$	199.59	1.19	–	–	19.23	6.9071	199.59	1.19	–	–	54,314.76	6.9076
	Logistic		1.06	–	−0.75	18.25	0.0099	200.42	1.06	–	−0.75	43,271.24	0.0104

Note: Empirical mean DW-at-birth (83.0 mm DW) was used in the $VBGF_{2par}$ model.
Abbreviation: DW, disc width; DW_∞

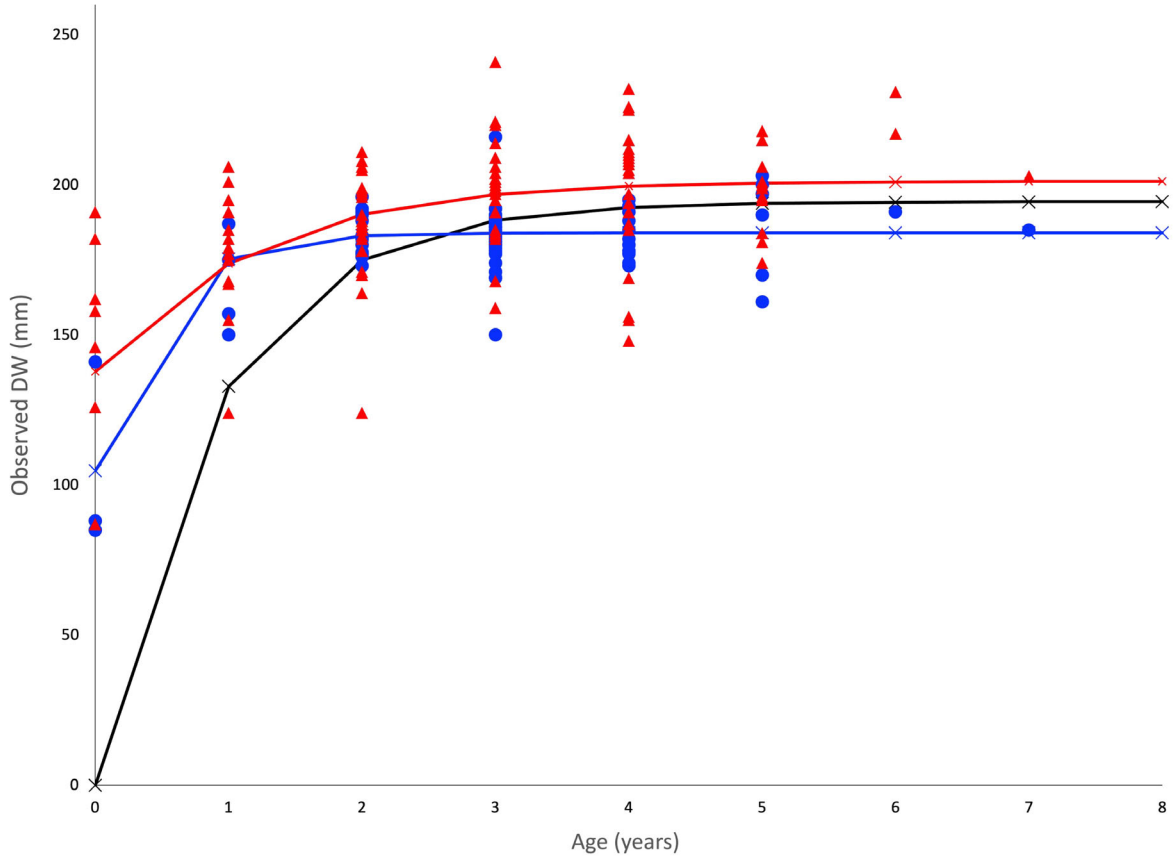

FIGURE 7 Selected growth curves of best-fit DW-at-age data for sexes combined, males and females. —×—, $VBGF_{mod}$ (SC); —×—, $VBGF_{2par}$ (M); —×—, Gompertz (F); ●, male; ▲, female

165 mm, 166–210 mm and 211–255 mm DW) showed no significant differences between months for both smaller size classes (120–165 mm DW and 166–210 mm DW) (ANOVA, $F_{6,6} = 2.41$, $P = 0.1541$; ANOVA, $F_{11,146} = 0.99$, $P = 0.4587$) (Supporting Information Figure S8). However, comparisons of the largest size class (211–255 mm DW) found statistical differences between months with a Tukey pair-wise comparison (ANOVA, $F_{9,7} = 4.58$, $P = 0.029$). Peaks occurred during January (1.730 ± 0, $n = 1$) while the lowest sample means occurred during June (0.313 ± 0, $n = 1$). There were monthly variations found for edge type (opaque *vs.* translucent bands) along the vertebral centra for yellow stingrays ($n = 121$). Opaque bands were recorded for the edge type during all months, with April having the highest count, whereas translucent bands were present during all months except April (Figure 6). Translucent bands occurred most frequently during March, May and June, while opaque bands were more prevalent through the rest of the year.

DW-at-age data were fit to growth models for samples with agreed-on ages for both sexes combined ($n = 134$) and separated (male $n = 47$ and female $n = 87$). An AICc value of <2 indicated substantial support for the selected model (Katsanevakis & Maravelias, 2008). Our results also indicated that for the sexes combined the $VBGF_{mod}$, $VBGF_{2par}$ and the logistic models all had similar parameter values for both ML- and LS-fitted models, but if selecting the absolute lowest AICc value then the $VBGF_{mod}$ was best fit to the data (Table 1 and Figure 7). The AICc for both ML- and LS-fitted models indicated a best fit of the $VBGF_{2par}$ for males (Table 1 and Figure 7), while all models with the exception of the $VBGF_{2par}$ was best fit for the female data (Table 1 and Figure 7).

4 | DISCUSSION

Elasmobranchs are typically characterized as having a K-selected growth strategy, making them susceptible to fisheries and other anthropogenic stressors, such as habitat degradation. However, the present study of yellow stingrays found them to reach sexual maturity early, produce young twice a year and have shorter lifespans than commonly described for elasmobranch fishes. Our results, along with those of similar species, suggest a more productive life-history strategy that may be more resilient to these pressures (Torres-Palacios *et al.*, 2019).

The sex ratio for males and females for the current study was equal, with males reaching sexual maturity later than females and females growing to larger maximum sizes than males to accommodate for reproductive condition than males. For males, the inflexion point of the CL–DW relationship was similar to the male maturity ogive

TABLE 2 Reported age-at-maturity, size-at-maturity and female fecundity for family urotrygonidae species

Species	Sex	Size at maturity (mm)	Age at 50% Maturity (years)	Maximum age (years)	Female fecundity	Source
Urotrygon chilensis	M	246 (TL)	4.3	12	–	Guzman-Castellanos, 2015
	F	258 (TL)	4.3	14	5	
Urotrygon aspidura	M	–	2.2	5.5	–	Torres-Palacios *et al*., 2019
	F	138–150 (DW)	2.3	7.5	4	
Urotrygon rogersi	M	118 (DW)	0.9	6	–	Mejía-Falla *et al*., 2014
	F	118–123 (DW)	1	8	3	
Urotrygon microphthalmum	M	183 (TL)	2	9	–	Santander-Neto *et al*., 2016
	F	199 (TL)	2	9	4	
Urobatis jamaicensis	M	154 (DW)	0.65	5	–	Current Study; Fahy, 2017
	F	157 (DW)	0.68	6	7	
Urobatis halleri	M	150 (DW)	3.75	14	–	Hale & Lowe, 2008
	F	150 (DW)	3.8	14	11	
Urobatis concentricus	M	–		4	–	Ehemann *et al*., 2017
	F	–	3	4	3	
Dasyatis pastinaca	M	83 (TL)	6.3	10	–	Yigin & Ismen, 2012
	F	114 (TL)	6.5	16	–	
Hypanus dipterurus	M	465 (DW)	6.4	25	–	Smith *et al*., 2007
	F	573 (DW)	8.3	28	3	
Bathytoshia lata	M	749 (DW)	8.3	25	--	Dale & Holland, 2012
	F	1049 (DW)	15	28	–	

Note: DW, disc width; F, female; M, male; TL, total length.

(DW_{50}). The negligible difference between the two analyses strongly supported the size at maturity ogives, although a larger sample size for males with DW sizes between 130 and 145 mm DW remains necessary to rule out a smaller size at maturity. Previous studies have suggested that male yellow stingrays reach sexual maturity *ca*. 200 mm TL (Sulikowski, 1996; Yañez-Arancibia & Amezcua-Linares, 1979). Related urotrygonids such as male *Urobatis halleri* (Hale & Lowe, 2008) and *U. rogersi* (Mejía-Falla *et al*., 2012) have been recorded as sexually mature at 150 and 118 mm DW, respectively (Table 2 and Figure 8). Previous literature on female *U. jamaicensis* by Yañez-Arancibia and Amezcua-Linares (1979) and Sulikowski (1996) suggests sexual maturity also peaks at *ca*. 200 mm TL (*ca*. 116 mm DW, unpublished data). Like the males, other female urotrygonids had a range of similar sizes-at-first maturity with 150 mm and 118 mm DW (Hale & Lowe, 2008; Mejía-Falla *et al*., 2012) (Table 2 and Figure 8). Females grow slower and larger, and live longer than males to accommodate the higher energetic costs of reproduction and larger brood sizes. This strategy, which is typical for viviparous elasmobranchs, may result from a biological adaptation influenced by reproduction rather than environmental factors (Mejía-Falla *et al*., 2014).

Despite similar batoid species having a generally larger age-at-first maturity estimate, yellow stingrays reaching sexual maturity within the first year would not be unrealistic as they are a fast-growing, short-lived, tropical species. The only other batoid species to our knowledge with a recorded age-at-first maturity <1 year is *U. rogersi*, a related species with a proposed triannual reproductive cycle and maximum age estimates of 8 and 11 years old for males and females, respectively (Mejía-Falla *et al*., 2014). Although *U. rogersi* is described as having a triannual cycle, it may not produce three broods per year, but rather have an asynchronous cycle with three peaks per year. This difference in frequency of birth could affect the differences in maximum ages achieved between the species.

The positive relationship between V_R and DW indicated its usefulness for age-estimations, as growth of the vertebral centra remained proportional with somatic growth (Dale & Holland, 2012; Mejía-Falla *et al*., 2014; Sulikowski, 1996). There were significant differences between males and females, which have been similarly reported for other myliobatiform rays, with females growing larger to accommodate reproductive condition and larger brood sizes (Almeida *et al*., 2000; Hazin *et al*., 2006; Mejía-Falla *et al*., 2012; White *et al*., 2001). Mejía-Falla *et al*. (2012) noted that female *Urotrygon rogersi* will reach larger sizes and masses than males but reach sexual maturity at a similar size and age, like *Trygoptera personata* (White *et al*., 2001) or *U. jamaicensis* in the current study.

Evidence of annual band deposition for combined size classes was inconclusive, whereas individual size classes (120–165 mm, 166–210 mm and 211–255 mm DW) revealed that larger yellow stingrays had more of an annual pattern of band deposition with opaque growth (thicker bands) during January and translucent growth (thinner bands) during June and August. Previous literature suggests that

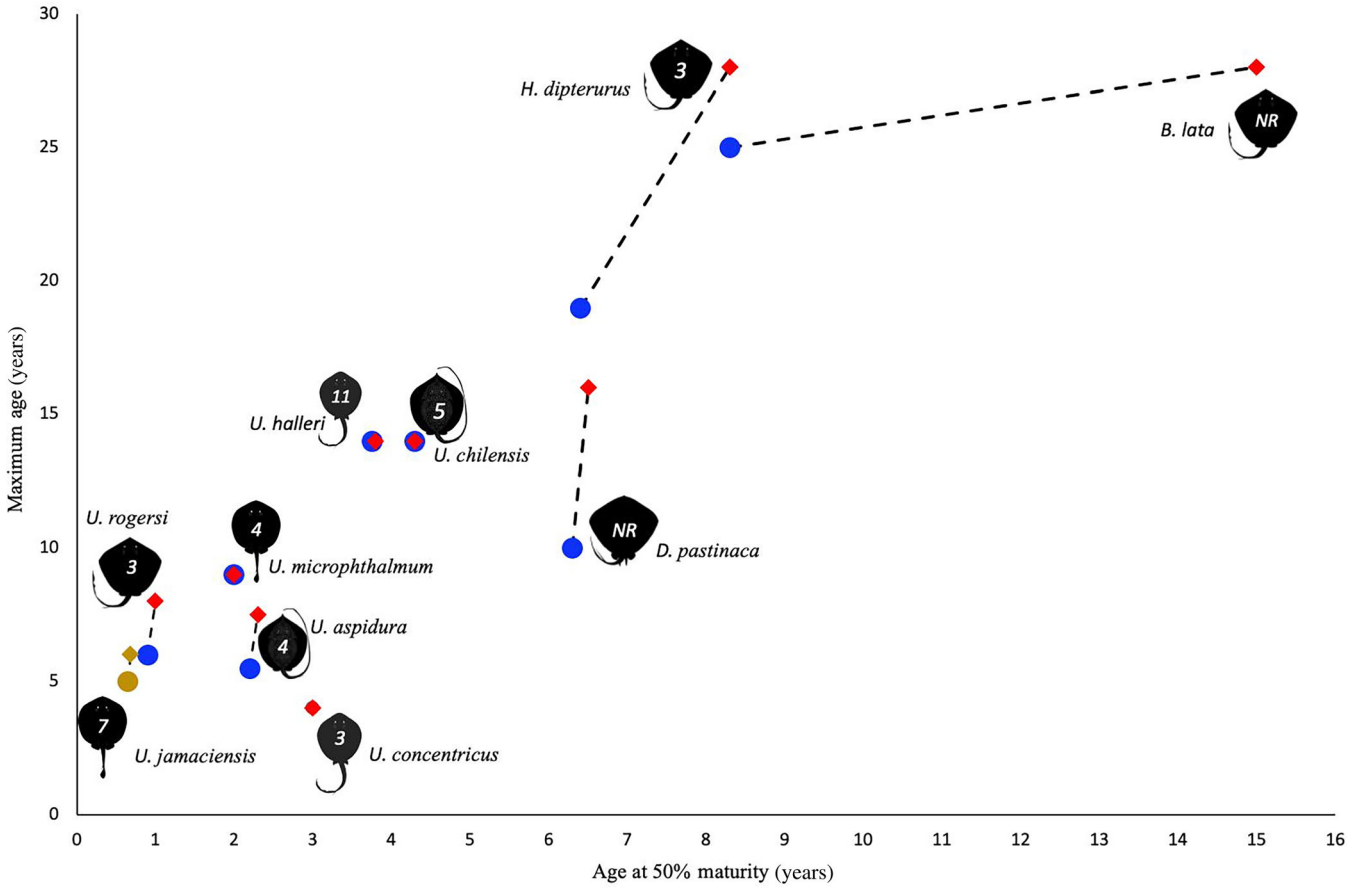

FIGURE 8 Reported age-at-maturity, maximum age and female fecundity (indicated by numbers within stingray shape; NR indicates fecundity not reported) for similar Myliobatid species. ●, male; ◆, female

variations in band deposition are possible over time as changes along the vertebral column due to both ontogeny and somatic growth can affect the deposition rate of band pairs (Huveneers *et al*., 2013; Natanson *et al*., 2008; Natanson, Andrews, *et al*., 2018; Natanson, Skomal, *et al*., 2018). A species of wobbegong shark found in western Australia (*Orectolobus hutchinsi*) has similar band deposition patterns. Neonates were reported to produce up to three growth bands per year, while adults produced less than one band per year, supporting the theory of a nonseasonal somatic growth influence with larger vertebrae having more consistent growth band deposition (Chidlow *et al*., 2007; Huveneers *et al*., 2013). For yellow stingrays, there is an obvious variation in band deposition rate within the first few years of life. Considering that yellow stingrays reproduce biannually with ovulation coinciding with parturition, energy resources allocated towards somatic growth versus reproduction may vary greatly, especially at young ages where small sizes may affect mating behaviour and brood size. Typically, with the onset of maturity, the energy allocated towards growth is reduced and maximum size reaches an asymptote (Mejía-Falla *et al*., 2014). It was noticed for yellow stingrays that maturity occurs early, but growth may only slow down rather than plateau as age increases. The benefits of this strategy could influence recovery potential from the elevated mortality risks caused by habitat changes, high predation from larger predators or fishing pressures, including collections for the aquarium trade (Baje *et al*., 2018). When comparing the edge analysis with the reproductive cycle, March peaks in ovulation during the first cycle coincided with a higher percentage of translucent band growth, suggesting resource allocation may be focused more towards vitellogenesis and ovulation rather than growth. Conversely, during the second cycle, which is characterized by smaller brood sizes but larger embryos, peaks in ovulation that occurred during August/September coincided with more opaque bands, suggesting resources may be allocated towards growth rather than vitellogenesis and ovulation. During both cycles, an increase in opaque growth occurred during April and November, subsequent to the onset of gestation (Fahy, 2004, 2017).

Despite the evidence of edge analysis following the biannual reproductive pattern noted through the literature for yellow stingrays, a biannual pattern in growth band formation was not statistically evident for the marginal increment analysis. However, if visually assessing MIA, a biannual pattern of growth may be discernible, with peaks between February and April and again in August which coincide with the cease of ovulation in larger female stingrays. However, the trade-offs of energy allocation between somatic growth and reproduction in yellow stingrays may influence the deposition of band pairs, leading to nonannual growth marks along the vertebral centra.

The majority of age-estimation studies may solely depend on the use of a selected *a priori* single model such as the original VBGF, which in some cases may not be fully supported by the data or the growth trajectory of a species (Katsanevakis & Maravelias, 2008). The use of multiple growth models provides a more robust approach to estimates of different growth parameters that are typically unavailable, such as DW_0, and lowers the risk of yielding biologically unrealistic growth estimates (Katsanevakis & Maravelias, 2008; Smart *et al*., 2016). Size-at-age data was fit to the five different growth models using the LS regression technique and the ML technique. Both suggest that females grow slower than males but reach larger maximum sizes, as indicated by the *k* and DW_∞ values or how quickly (*k*) the stingrays approach the maximum mean DW (DW_∞) (Ogle, 2016). AICc values further suggest that the two-parameter von Bertalanffy model best fits the male data, while the Gompertz model ultimately best fits the female data. Although not included within the present study, the use of a multimodel inference by model averaging based on 'Akaike weights' may have provided a more precise estimation of model parameters and eliminated model uncertainty from multiple models producing viable parameters (Katsanevakis & Maravelias, 2008).

Despite male rays having a larger *k* value, similar or smaller DW_∞ values were found when compared with related species. For example, *U. rogersi* has a triannual, aseasonal reproductive pattern. To account for this pattern, Mejía-Falla *et al*. (2014) adjusted age by averaging the time between birth and first band formation and found a two-phase growth function with a DW_∞ of 155 mm and a *k* value of 0.65 $year^{-1}$.These adjustments could account for the drastic differences in *k* values between *U. rogersi* and *U. jamaicensis*. Hale and Lowe (2008) studied the growth rates for *U. halleri* through wild collected samples and samples held in captivity that were injected with oxytetracycline (OTC), and noted a DW_∞ of 286 mm and a *k* value of 0.09 $year^{-1}$ for *U. halleri*. Although *U. halleri* displayed annual periodicity along the vertebral centra with the OTC injections, growth rates could have been affected by captivity despite constant habitat conditions (Huveneers *et al*., 2013). Branstetter (1990) described growth rates as being slow if *k* was <1 $year^{-1}$ or considerably fast if >1 $year^{-1}$, indicating that yellow stingrays would be considered a comparably fast-growing species with a *k* value of 1.15 $year^{-1}$ for sexes combined. Other than the obvious variations caused by species differences, factors such as habitat type, sample size, ageing methodology, validation method and model fitting can also lead to variation in the growth rates of closely related species (Cailliet & Goldman, 2004; Smith *et al*., 2007). Regardless of all these influential factors, *k* can still provide a practical characterization of the rudimentary factors associated with fecundity, longevity and size or age at maturity (Smith *et al*., 2007; Stearns, 1982).

The growth patterns and consecutive 6-month reproductive cycles found for yellow stingrays may account for the variations in birth date, a lack of age validation before the age of three, the variations between MIA and edge analysis, and the large growth rate coefficient (*k*) determined in the growth models. Seasonality in growth band formation is typically associated with the seasonal variations in environmental variables such as temperature and the availability of resources. Tropical elasmobranchs are generally thought to lack seasonality in growth patterns due to the constancy of the tropical environment. Although sea water temperatures for these environments can vary significantly, resource availability associated with seasonal rainfall (*i.e*., wet and dry seasons) has been considered the primary driver of phenological patterns (Green *et al*., 2009). Yellow stingrays seem to have higher growth during the dry winter months and slower growth in the wet summer months. This seasonality in growth for females could be due to females having increased fecundity, smaller embryos and slower growth during the spring/summer months and decreased fecundity, faster growth and larger embryo sizes during the fall/winter months. Larger brood sizes with smaller sized offspring during the first cycle occurred during the summer months, when water temperature was elevated (Fahy, 2004; Fahy *et al*., 2007). Male yellow stingrays have biannual peaks in sperm production that precede the ovulatory patterns in females by 1–2 months (Fahy, 2017). Males are recorded more frequently in the same areas as females during the post-partum/pre-ovulatory periods, follow similar peaks in reproductive patterns as females and thus possibly have similar peaks in growth patterns.

The growth and reproduction patterns for yellow stingrays within this study may also be influenced by the distinct water temperature patterns associated with the increasing and decreasing light regime for the subtropical environment in which they were sampled. These temperature changes may influence the endocrine patterns for this species, leading to the increased winter growth and decreased summer growth patterns found. Further support for this hypothesis includes the composition of the vertebral bands themselves. According to Green *et al*. (2009), calcified opaque bands and protein-rich translucent bands occur within fish otoliths, a hard part structure used to age teleost fishes. If the opaque and translucent bands follow a similar composition to that of fish otoliths, then the protein-rich translucent bands occurring most often during yellow stingray peak ovulation could explain the thin bands occurring during the spring and summer months when fecundity is highest.

The yellow stingray is a small, fast-growing urotrygonid that reaches more than 40% of asymptotic size by birth and attains an estimated maximum of 5 and 6 years of age for males and females, respectively. Although males and females have similar sizes at maturity, males grow faster and mature at a younger age, whereas females grow slower but achieve larger maximum sizes. The annual periodicity of band pairs could only be verified with marginal increment analysis and edge analysis for larger stingrays. These patterns support rapid growth through the first few years of life, followed by slower, more consistent growth as age and size increased. These patterns suggest growth rates are most likely attributed to nonannual somatic growth rather than seasonality. Growth estimates for both male and female stingrays yielded large *k* values and small DW_∞ estimates, which are both consistent with a short-lived, fast-growing tropical batoid. Considering only seven of the 20 known species within the Urotrygonidae family have sexual maturity and age information available, the results of this study can be used to fill in the knowledge gaps for similar species. The age and growth data collected from this study could also be used as a proxy for ecosystem-based management decisions of similar

small, tropical, or fishery-impacted batoid, as well as providing a diverse outlook for data-deficient species or species that may display a nonannual or nonseasonal somatic growth pattern.

AUTHOR CONTRIBUTIONS

All persons who meet authorship criteria are listed as authors. Conception and design of study: J.J.S. and D.W.K. Data generation: J.J.S. and D.P.F. Data analysis: J.J.S., D.P.F., J.K.C. and D.W.K. Manuscript preparation: J.J.S., D.P.F., J.K.C. and D.W.K. Although the work did not receive any internal or external funding, equipment and supplies were provided by D.W.K.

ACKNOWLEDGEMENTS

We would like to thank all that helped and supported this research, including Matthew Dancho, Patrick Lynch, Lisa J. Natanson, Kelsey James, Jacquelyn Reuder and Caroline Collatos during processing and analysis. We also thank Alexander Rayburn for creating the supplemental map figure. Specimens were collected under NSU IACUC #2019.08.DK4 and a Special Activities Licence (SAL-17-1947-SR) from the Florida Fish and Wildlife Conservation Commission (FWC). The scientific results and conclusions, as well as any views or opinions expressed herein are those of the author(s) and do not necessarily reflect those of their institutions or agencies.

FUNDING INFORMATION

The research did not receive any internal or external funding.

ORCID

Jessica J. Schieber https://orcid.org/0000-0001-7623-4717
Daniel P. Fahy https://orcid.org/0000-0002-1504-4247
John K. Carlson https://orcid.org/0000-0001-8205-6558
David W. Kerstetter https://orcid.org/0000-0002-4440-8767

REFERENCES

Abràmoff, M. D., Magalhães, P. J., & Ram, S. J. (2004). Image processing with ImageJ. *Biophotonics International*, *11*(7), 36–42 https://dspace.library.uu.nl/handle/1874/204900.

Ainsley, S. M. (2009). *Age, growth and reproduction of the Bering Skate, Bathyraja interrupta (Gill and Townsend, 1897), from the eastern Bering Sea and Gulf of Alaska* (MS thesis). Monterey Bay: California State University Available from: https://scholarworks.calstate.edu/downloads/z890rz92r.

Almeida, Z. S., Nunes, J. S., & Costa, C. L. (2000). Presencia de *Urotrygon microphthalmum* (Elasmobranchii: Urolophidae) en aguas bajas de Maranhao (Brasil) y notas sobre su biología. *Boletin de Investigaciones Marinas y Costeras*, *29*, 67–72 https://hdl.handle.net/1834/3429.

Baje, L., Smart, J. J., Chin, A., White, W. T., & Simpfendorfer, C. A. (2018). Age, growth and maturity of the Australian sharpnose shark *Rhizoprionodon taylori* from the Gulf of Papua. *PLoS One*, *13*(10), e0206581. https://doi.org/10.1371/journal.pone.0206581.

Başusta, N., & Aslan, E. (2018). Age and growth of bull ray *Aetomylaeus bovinus* (Chondrichthyes: Myliobatidae) from the northeastern Mediterranean coast of Turkey. *Cahiers de Biologie Marine*, *59*(1), 107–114. https://doi.org/10.21411/cbm.a.5f77152e.

Bowker, A. H. (1948). A test for symmetry in contingency tables. *Journal of the American Statistical Association*, *43*(244), 572–574. https://doi.org/10.1080/01621459.1948.10483284.

Branstetter, S. (1990). Early life-history implications of selected carcharhinid and lamnoid sharks of the Northwest Atlantic. In H. L. Pratt, S. H. Gruber, & T. Taniuchi (Eds.), *Elasmobranchs as living resources: Advances in the biology* (pp. 17–28). Silver Spring, MD, USA: Ecology, Systematics, and the Status of the Fisheries.

Cailliet, G. (2015). Perspectives on elasmobranch life-history studies: A focus on age validation and relevance to fishery management. *Journal of Fish Biology*, *87*(6), 1271–1292. https://doi.org/10.1111/jfb.12829.

Cailliet, G. M. (1990). Elasmobranch age determination and verification: An updated review. In H. L. Pratt, S. H. Gruber, & T. Taniuchi (Eds.), *Elasmobranchs as living resources: Advances in the biology, ecology, systematics, and the status of the fisheries* (pp. 157–165). Silver Spring, MD, USA: National Marine Fisheries Service.

Cailliet, G. M., & Goldman, K. J. (2004). Age determination and validation in chondrichthyan fishes. In J. C. Carrier, J. A. Musick, & M. R. Heithaus (Eds.), *Biology of sharks and their relatives* (Vol. 2004, pp. 399–447). Boca Raton, FL, USA: CRC Press.

Cailliet, G. M., Smith, W. D., Mollet, H. F., & Goldman, K. J. (2006). Age and growth studies of chondrichthyan fishes: The need for consistency in terminology, verification, validation, and growth function fitting. *Environmental Biology of Fishes*, *77*(3), 211–228. https://doi.org/10.1007/s10641-006-9105-5.

Campana, S. (2001). Accuracy, precision and quality control in age determination, including a review of the use and abuse of age validation methods. *Journal of Fish Biology*, *59*(2), 197–242. https://doi.org/10.1006/jfbi.2001.1668.

Campana, S. E. (2014. Available from:). *Age determination of elasmobranchs, with special reference to Mediterranean species: A technical manual (internet)*. Rome: UN Food and Agriculture Organization. https://www.fao.org/3/i3762e/i3762e.pdf.

Campana, S. E., Annand, M. C., & McMillan, J. I. (1995). Graphical and statistical methods for determining the consistency of age determinations. *Transactions of the American fisheries Society*, *124*(1), 131–138. https://doi.org/10.1577/1548-8659(1995)124<0131:GASMFD>2.3.CO;2.

Castellanos, A. B. G. (2015). *Historia de vida de la raya chilena Urotrygon chilensis (Günther, 1872) en el sureste del Pacífico mexicano*. [Ph.D. dissertation]. S.C: Centro de Investigaciones Biológicas del Noroeste Avaiable from: http://dspace.cibnor.mx:8080/handle/123456789/475.

Charvet, P., Santana, F., De Lima, K., & Lessa, R. (2018). Age and growth of the endemic Xingu River stingray *Potamotrygon leopoldi* validated using fluorescent dyes. *Journal of Fish Biology*, *92*(6), 1985–1999. https://doi.org/10.1111/jfb.13635.

Chidlow, J. A., Simpfendorfer, C. A., & Russ, G. R. (2007). Variable growth band deposition leads to age and growth uncertainty in the western wobbegong shark, Orectolobus hutchinsi. *Marine and Freshwater Research*, *58*(9), 856–865. https://doi.org/10.1071/MF06249.

Christiansen, H. M., Campana, S. E., Fisk, A. T., Cliff, G., Wintner, S. P., Dudley, S. F., et al. (2016). Using bomb radiocarbon to estimate age and growth of the white shark, *Carcharodon carcharias*, from the southwestern Indian Ocean. *Marine Biology*, *163*(6), 1–13. https://doi.org/10.1007/s00227-016-2916-9.

Coelho, R., & Erzini, K. (2005). Length at first maturity of two species of lantern sharks (*Etmopterus spinax* and *Etmopterus pusillus*) from southern Portugal. *Journal of the Marine Biological Association of the UK*, *85*(5), 1163–1165. https://doi.org/10.1017/S0025315405012245.

Cotton, C. F., Grubbs, R. D., Daly-Engel, T. S., Lynch, P. D., & Musick, J. A. (2011). Age, growth and reproduction of a common deep-water shark, shortspine spurdog (*Squalus cf. mitsukurii*), from Hawaiian waters. *Marine and Freshwater Research*, *62*(7), 811–822. https://doi.org/10.1071/MF10307.

Dale, J., & Holland, K. (2012). Age, growth and maturity of the brown stingray (*Dasyatis lata*) around Oahu, Hawai'i. *Marine and Freshwater Research*, *63*(6), 475–484. https://doi.org/10.1071/MF11231.

Davis, C. D., Cailliet, G. M., & Ebert, D. A. (2007). Age and growth of the roughtail skate Bathyraja trachura (Gilbert, 1892) from the eastern North Pacific. *Environmental Biology of Fishes*, *80*, 325–326. https://doi.org/10.1007/s10641-007-9224-7.

Dulvy, N. K., Fowler, S. L., Musick, J. A., Cavanagh, R. D., Kyne, P. M., Harrison, L. R., … White, W. T. (2014). Extinction risk and conservation of the world's sharks and rays. *eLife*, *3*, e00590 https://elifesciences.org/articles/00590.pdf.

Ehemann, N. R., Pérez-Palafox, X. A., Pabón-Aldana, K., Mejía-Falla, P. A., Navia, A. F., & Cruz-Escalona, V. H. (2017). Biological notes on the reef stingray, *Urobatis concentricus*, an endemic species of Mexico. *Journal of Fish Biology*, *91*(4), 1228–1235. https://doi.org/10.1111/jfb.13398.

Evans, G. T., & Hoenig, J. M. (1998). Testing and viewing symmetry in contingency tables, with application to readers of fish ages. *Biometrics*, *54*, 620–629. https://doi.org/10.2307/3109768.

Fahy, D. P. (2004). *Diel activity patterns, space utilization, seasonal distribution and population structure of the yellow stingray, Urobatis jamaicensis (Cuvier, 1817) in South Florida with comments on reproduction*. (MS thesis). Fort Lauderdale, FL, USA: Nova Southeastern University. Available from: https://nsuworks.nova.edu/occ_stuetd/121.

Fahy, D. P. (2017). *The biannual cycle and reproductive morphology of the yellow stingray, Urobatis jamaicensis (Cuvier, 1817), with a comparative analysis from batoid reproductive literature*. (Ph.D. dissertation). Dania Beach, FL, USA: Nova Southeastern University. Available from: https://nsuworks.nova.edu/occ_stuetd/455.

Fahy, D. P., Spieler, R. E., & Hamlett, W. C. (2007). Preliminary observations on the reproductive cycle and uterine fecundity of the yellow stingray, *Urobatis jamaicensis* (Elasmobranchii: Mylioba tiformes: Urolophidae) in Southeast Florida, USA. *Raffles Bulletin of Zoology*, *14*, 131–139. Available from https://nsuworks.nova.edu/occ_facarticles/154.

Fernandez-Carvalho, J., Coelho, R., Erzini, K., & Santos, M. N. (2011). Age and growth of the bigeye thresher shark, *Alopias superciliosus*, from the pelagic longline fisheries in the tropical northeastern Atlantic Ocean, determined by vertebral band counts. *Aquatic Living Resources*, *24*(4), 359–368. https://doi.org/10.1051/alr/2011046.

Ferrette, B. L. S., Domingues, R. R., Rotundo, M. M., Miranda, M. P., Bunholi, I. V., De Biasi, J. B., … Mendonça, F. F. (2019). DNA barcode reveals the bycatch of endangered batoids species in the Southwest Atlantic: Implications for sustainable fisheries management and conservation efforts. *Genes-Basel*, *10*(304), 1–15. https://doi.org/10.3390/genes10040304.

Gianeti, M. D., Santana, F. M., Yokota, L., Vasconcelos, J. E., Dias, J. F., & Lessa, R. P. (2019). Age structure and multi-model growth estimation of longnose stingray *Hypanus guttatus* (Dasyatidae: Myliobatoidei) from north-East Brazil. *Journal of Fish Biology*, *94*(3), 481–488. https://doi.org/10.1111/jfb.13918.

Green, B. S., Mapstone, B. D., Carlos, G., & Begg, G. A. (Eds.). (2009). *Tropical fish otoliths: Information for assessment, management and ecology*. New York, NY: Springer.

Hale, L. F., & Lowe, C. (2008). Age and growth of the round stingray *Urobatis halleri* at Seal Beach. *California. J Fish Biol.*, *73*(3), 510–523. https://doi.org/10.1111/j.1095-8649.2008.01940.x.

Hale, L. F., Dudgeon, J. V., Mason, A. Z., & Lowe, C. G. (2006). Elemental signatures in the vertebral cartilage of the round stingray, *Urobatis halleri*, from Seal Beach, California. *Environmental Biology of Fishes*, *77*, 317–325. https://doi.org/10.1007/s10641-006-9124-2.

Hayne, A. H., Poulakis, G. R., Seitz, J. C., & Sulikowski, J. A. (2018). Preliminary age estimates for female southern stingrays (*Hypanus americanus*) from southwestern Florida, USA. Gulf and Caribbean. *Research*, *29*(1), SC1-SC4. https://doi.org/10.18785/gcr.2901.03.

Hazin, F. H., Fischer, A. F., Broadhurst, M. K., Veras, D., Oliveira, P. G., & Burgess, G. H. (2006). Notes on the reproduction of *Squalus megalops* off northeastern Brazil. *Fisheries Research*, *79*(3), 251–257. https://doi.org/10.1016/j.fishres.2006.04.006.

Huveneers, C., Stead, J., Bennett, M. B., Lee, K. A., & Harcourt, R. G. (2013). Age and growth determination of three sympatric wobbegong sharks: How reliable is growth band periodicity in Orectolobidae? *Fisheries Research*, *147*, 413–425. https://doi.org/10.1016/j.fishres.2013.03.014.

Katsanevakis, S., & Maravelias, C. D. (2008). Modelling fish growth: Multi-model inference as a better alternative to a priori using von Bertalanffy equation. *Fish and Fisheries*, *9*(2), 178–187. https://doi.org/10.1111/j.1467-2979.2008.00279.x.

Kyne, P. M., Carlson, J. K., Ebert, D. A., Fordham, S. V., Bizzarro, J. J., Graham, R. T., … Dulvy, N. K. (Eds.). (2012). *The conservation status of north American, central American, and Caribbean chondrichthyans*. IUCN Species Survival Commission Shark Specialist Group: Vancouver.

Lessa, R., Santana, F. M., & Duarte-Neto, P. (2006). A critical appraisal of marginal increment analysis for assessing temporal periodicity in band formation among tropical sharks. *Environmental Biology of Fishes*, *77*(3), 309–315. https://doi.org/10.1007/s10641-006-9111-7.

Matta, M. E., Tribuzio, C. A., Ebert, D. A., Goldman, K. J., & Gburski, C. M. (2017). Age and growth of elasmobranchs and applications to fisheries management and conservation in the Northeast Pacific Ocean. *Advances in Marine Biology*, *77*, 179–220. https://doi.org/10.1016/bs.amb.2017.06.002.

McAuley, R. B., Simpfendorfer, C. A., Hyndes, G. A., Allison, R. R., Chidlow, J. A., Newman, S. J., & Lenanton, R. C. (2006). Validated age and growth of the sandbar shark, *Carcharhinus plumbeus* (Nardo 1827) in the waters off Western Australia. *Environmental Biology of Fishes*, *77*, 385–400. https://doi.org/10.1007/s10641-006-9126-0.

McNemar, Q. (1947). Note on the sampling error of the difference between correlated proportions or percentages. *Psychometrika*, *12*(2), 153–157. https://doi.org/10.1007/BF02295996.

Mejía-Falla, P. A., Cortés, E., Navia, A. F., & Zapata, F. A. (2014). Age and growth of the round stingray *Urotrygon rogersi*, a particularly fast-growing and short-lived elasmobranch. *PLoS One*, *9*(4), e96077. https://doi.org/10.1371/journal.pone.0096077.

Mejía-Falla, P., Navia, A., & Cortés, E. (2012). Reproductive variables of *Urotrygon rogersi* (Batoidea: Urotrygonidae): A species with a triannual reproductive cycle in the eastern tropical Pacific Ocean. *Journal of Fish Biology*, *80*(5), 1246–1266. https://doi.org/10.1111/j.1095-8649.2012.03237.x.

Mollet, H., Ezcurra, J., & O'sullivan, J. (2002). Captive biology of the pelagic stingray, *Dasyatis violacea* (Bonaparte, 1832). *Marine and Freshwater Research*, *53*(2), 531–541. https://doi.org/10.1071/MF01074.

Natanson, L. J., & Cailliet, G. M. (1990). Vertebral growth zone deposition in Pacific angel sharks. *Copeia*, *1190*(4), 1133–1145. https://doi.org/10.2307/1446499.

Natanson, L. J., Andrews, A. H., Passerotti, M. S., & Wintner, S. P. (2018). History and mystery of age and growth studies in elasmobranchs. In J. C. Carrier & M. R. Heithaus (Eds.), *Simpfendorfer CA, editors* (pp. 177–200). Shark Research: Emerging Technologies and Applications for the Field and Laboratory.

Natanson, L. J., Gervelis, B. J., Winton, M. V., Hamady, L. L., Gulak, S. J., & Carlson, J. K. (2014). Validated age and growth estimates for *Carcharhinus obscurus* in the northwestern Atlantic Ocean, with pre-and post management growth comparisons. *Environmental Biology of Fishes*, *97*(8), 881–896. https://doi.org/10.1007/s10641-013-0189-4.

Natanson, L. J., Skomal, G. B., Hoffmann, S. L., Porter, M. E., Goldman, K. J., & Serra, D. (2018). Age and growth of sharks: Do vertebral band pairs record age? *Marine and Freshwater Research*, *69*(9), 1440–1452. https://doi.org/10.1071/MF17279.

Natanson, L. J., Wintner, S. P., Johansson, F., Piercy, A., Campbell, P., De Maddalena, A., … Hemida, F. (2008). Ontogenetic vertebral growth patterns in the basking shark *Cetorhinus maximus*. *Marine Ecology Progress Series*, *361*, 267–278. https://doi.org/10.3354/meps07399.

O'Shea, O. R., Braccini, M., McAuley, R., Speed, C. W., & Meekan, M. G. (2013). Growth of tropical dasyatid rays estimated using a multi-

analytical approach. *PLoS One*, *8*(10), e77194. https://doi.org/10.1371/journal.pone.0077194.

Ogle, D. H. (2016). *Introductory fisheries analyses with R*. Boca Raton: Chapman and Hall/CRC Press.

Okamura, H., & Semba, Y. (2009). A novel statistical method for validating the periodicity of vertebral growth band formation in elasmobranch fishes. *Canadian Journal of Fisheries and Aquatic Sciences*, *66*(5), 771–780. https://doi.org/10.1139/F09-039.

Okamura, H., Punt, A., Semba, Y., & Ichinokawa, M. (2013). Marginal increment analysis: A new statistical approach of testing for temporal periodicity in fish age verification. *Journal of Fish Biology*, *82*(4), 1239–1249. https://doi.org/10.1111/jfb.12062.

Oliver, S., Braccini, M., Newman, S. J., & Harvey, E. S. (2015). Global patterns in the bycatch of sharks and rays. *Marine Policy*, *54*, 86–97. https://doi.org/10.1016/j.marpol.2014.12.017.

Parsons, K., Maisano, J., Gregg, J., Cotton, C., & Latour, R. (2018). Age and growth assessment of western North Atlantic spiny butterfly ray *Gymnura altavela* (L. 1758) using computed tomography of vertebral centra. *Environmental Biology of Fishes*, *101*(1), 137–151. https://doi.org/10.1007/s10641-017-0687-x.

Santander-Neto, J., Araújo, M. L. G., & Lessa, R. (2016). Reproductive biology of *Urotrygon microphthalmum* (Batoidea: Urotrygonidae) from North-Eastern Brazil, tropical West Atlantic Ocean. *Journal of Fish Biology*, *89*(1), 1026–1042. https://doi.org/10.1111/jfb.12951.

Schneider, C. A., Rasband, W. S., & Eliceiri, K. W. (2012). NIH image to ImageJ: 25 years of image analysis. *Nature Methods*, *9*(7), 671–675. https://doi.org/10.1038/nmeth.2089.

Smart, J. J., Chin, A., Tobin, A. J., & Simpfendorfer, C. A. (2016). Multimodel approaches in shark and ray growth studies: Strengths, weaknesses and the future. *Fish and Fisheries*, *17*(4), 955–971. https://doi.org/10.1111/faf.12154.

Smith, W. D., Cailliet, G. M., & Melendez, E. M. (2007). Maturity and growth characteristics of a commercially exploited stingray, *Dasyatis dipterura*. *Marine and Freshwater Research*, *58*(1), 54–66. https://doi.org/10.1071/MF06083.

Spieler, R. E., Fahy, D. P., Sherman, R. L., Sulikowski, J. A., & Quinn, T. P. (2013). (2013). The yellow stingray, *Urobatis jamaicensis* (Chondrichthyes: Urotrygonidae): A synoptic review. *Caribbean Journal of Science*, *47*(1), 67–97. https://doi.org/10.18475/cjos.v47i1.a8.

Stearns, S. C. (1982). In J. T. Bonner (Ed.), *The role of development in the evolution of life histories* (pp. 237–258). Berlin Heidelberg: Springer.

Sulikowski, J. (1996). *A preliminary study of the population density, size distribution age and growth of the stingray, Urolophus jamaicensis, in southeastern Florida*. (M.S. thesis). Fort Lauderdale, FL, USA: Nova Southeastern University Available from: https://nsuworks-nova-edu.ezproxylocal.library.nova.edu/occ_stuetd/319.

TeamRStudio R. (2018). *Integrated development environment for R. (internet) version 1.1.46, computer software*. RStudio: Boston, MA Available from: https://www.rstudio.com.

Torres-Palacios, K., Mejia-Falla, P. A., Navia, A. F., Cruz-Escalona, V. H., Felix-Uraga, R., & Quinonez-Velazquez, C. (2019). Age and growth parameters of the Panamic stingray (*Urotrygon aspidura*). *Fishery Bulletin*, *117*(3), 169–180. https://doi.org/10.7755/FB.117.3.4.

Von Bertalanffy, L. (1938). A quantitative theory of organic growth (inquiries on growth laws. II). *Human Biology*, *10*(2), 181–213. Available from: http://www.jstor.org/stable/41447359.

Ward-Paige, C. A., Pattengill-Semmens, C., Myers, R. A., & Lotze, H. K. (2011). Spatial and temporal trends in yellow stingray abundance: Evidence from diver surveys. *Environmental Biology of Fishes*, *90*(3), 263–276. https://doi.org/10.1007/s10641-010-9739-1.

White, W., Platell, M., & Potter, I. (2001). Relationship between reproductive biology and age composition and growth in *Urolophus lobatus* (Batoidea: Urolophidae). *Marine Biology*, *138*(1), 135–147. https://doi.org/10.1007/s002270000436.

Yañez-Arancibia, A., & Amezcua-Linares, F. (1979). Ecologia de *Urolophus jamaicensis* (Cuvier) en laguna de terminos un sistema estuarino del golfo sur del golfo de Mexico. (PISCES: Urolophidae). *Anales del Centro de Ciencias del Mar y Limnologia, Universidad Nacional Autónoma de México.*, *6*(2), 123–136. Available from: http://biblioweb.tic.unam.mx/cienciasdelmar/centro/1979-2/articulo76.html.

Yigin, C. C., & Ismen, A. (2012). Age, growth and reproduction of the common stingray, *Dasyatis pastinaca* from the North Aegean Sea. *Marine Biology Research*, *8*(7), 644–653. https://doi.org/10.1080/17451000.2012.659667.

SUPPORTING INFORMATION

Additional supporting information can be found online in the Supporting Information section at the end of this article.

How to cite this article: Schieber, J. J., Fahy, D. P., Carlson, J. K., & Kerstetter, D. W. (2023). Age, growth and maturity of the yellow stingray (*Urobatis jamaicensis*), a biannually reproductive tropical batoid. *Journal of Fish Biology*, 1–15. https://doi.org/10.1111/jfb.15374